Korean Journal of Chemical Engineering (2024) 41:2639–2650
https://doi.org/10.1007/s11814-024-00212-3

ORIGINAL ARTICLE

Production of Glycerol-Free Biodiesel Using Pollen-Derived CaO Heterogeneous Catalyst

Ying Tang[1,2] · Meng Li[1] · Guangtao Li[3] · Yi Yang[3] · Ying Yang[1]

Received: 24 March 2024 / Revised: 17 June 2024 / Accepted: 24 June 2024 / Published online: 2 July 2024

Abstract

Rape pollen with fishnet-like network structure has been used as support in the construction of high dispersion CaO materials assigned to CaO(P) ("P" was symbol of the precipitation method). Effect of various preparation conditions such as calcination temperature was evaluated following the performance for no-glycerol biodiesel preparation. The relatively well activity was observed by yielding to no-glycerol biodiesel of 92.69% in the rapeseed 1/1/8 mixture of oil–methyl acetate–methanol at 65 °C for 3 h over 10 wt% of 1/1-CaO(P)-700 which is better than 80% over commercial CaO. In addition, the catalytic performance of reused catalyst was also investigated. TGA–DSC and BET studies showed that the catalyst has good thermal stability and high surface area with hierarchical microstructures with large and mesopores on the surface, respectively. Furthermore, hierarchical basicity has been also established which provided various active sites for the heterogeneous reaction.

Keywords Biodiesel · Rape pollen · Precipitation method · Tri-component coupling transesterification · CaO

Introduction

Demand for the dieselization of vehicles has grown steadily due to the innovation of fuel market, which makes the promotion and development of diesel industry a focus attention [1]. Biodiesel, as a paradigm of biomass in the new era, has dual advantages, not only socially but also economically, from avoiding price fluctuations caused by traditional non-renewable fuels to realizing structural energy saving and emission reduction benefits [2]. However, the commercial petrochemical-diesel fuels are mainly derived from crude oil through a series of process methods such as distillation, catalytic cracking, thermal cracking, hydrocracking, and petroleum coking. Most of them are divided into hydrocarbons with carbon chain length concentrated between 12 and 25, which has the two major ailments of high sulfur and high nitrogen, severely shaking the construction of ecological civilization, especially its impact on the atmospheric environment [3, 4]. At present, the most common theory about biodiesel synthesis is based on the transesterification reaction developed by the two chemicals of triglyceride (TG) and methanol (MeOH) [5]. The as-synthetized biodiesel is of a low-carbon higher fatty acid composed of C, H and O, also known as the fatty acid methyl esters (FAME) with carbon chain lengths ranging from 16 to 20 [6]. However, the increase in biodiesel production increases the production of glycerin in a quantity much greater than the necessary demand. Therefore, the secondary utilization of glycerin resources has attracted extensive attention of the majority of researchers [7] by addition of the novel ester reagents to removal of by-product of glycerol [8]. In the common crafts, the assistance of homogeneous alkali (such as NaOH, KOH) or acid reagents (H_3PO_4, H_2SO_4) have been generally required, but the addition of such substances cause a consequence for the corrosion of equipment [9, 10]. The commodity oils could be obtained after neutralization, leading to the generation of the countless industrial wastewater, which does not accord well with the requirements of environmental catalysis. Calcium oxide with stronger alkalinity, low cost and low solubility in methanol, is one type of the potential alkaline earth metal oxides (H^- value: 10.1–11.1), which is

✉ Ying Tang
tangying78@xsyu.edu.cn

1 Shaanxi Engineering Research Center of Green Low-carbon Energy Materials and Processes, Xi'an Shiyou University, Xi'an, China

2 Xi'an Key Laboratory of Low-carbon Utilization for High-carbon Resources, Xi'an Shiyou University, Xi'an, China

3 Xi'an Petroleum JARN (Industrial) Group Co., Ltd., Xi'an, China

a solid base with commercial value and industrial prospects [11]. Therefore, the development of a green and efficient synthetic route for highly dispersed calcium oxide is of profound significance to solve the problem of energy shortage.

In previous research, templates have attracted great attention for preparing porous materials with uniform particle and well dispersion by controlling the growth of crystalline by preventing active species aggregation even under high calcination temperature during the removal process of template [12]. In addition to physical and chemical templates, a great deal of biologically functional tissues from nature could also provide new inspiration for modern material science and chemical reactions, ranging from insect wings, pollen grains, plant fiber, paper and eggshell membranes to bacteria, DNA, viruses, etc. [13]. Pollen has a rich porous structure and large specific surface area, and its outer wall has reticulated cavities with a large amount of proteins and phospholipids, which are easy to attach precursors and provide a medium for the doping of heteroelements [14]. Chen et al. [15] employed five distinct natural plant pollens (lotus, camellia, rapeseed, schisandra, and pine flower) as biological templates to synthesize anatase TiO_2 hollow spheres, thereby enhancing the photocatalytic performance of multiple rare-earth elements with both single and combined doping. The precipitation method is one of the most common ways in preparing solid catalysts, which refers to the employment of the precipitation agent (NaOH, Na_2CO_3) in the aqueous solution containing the metal salt under the control of a certain temperature and pH, to the formation of metal salt precipitation, such as hydrous oxide, carbonate crystals or gels. Subsequently, the as-obtained powder could be obtained by a series of processes, such as wash, dry, and calcination [16].

Since the critical factor in the synthesis of solid base materials is to tailor and control dispersion, the aim of the present work is to develop the precipitation approach based on pollen to prepare high dispersed CaO for enhanced no-glycerol biodiesel preparation by tri-component coupling transesterification. Meanwhile, the templated CaO(P) was also characterized to reveal its structure and properties.

Materials and Methods

Experimental Process

Solid-based CaO (P) was distributed in a mixing flask equipped with refined rapeseed oil, methyl acetate and methanol and refluxed under a magnetic stirrer at moderate temperature (65 °C) for 3.5 h. Then, centrifugation and rotary evaporation were done to complete the glycerol-free biodiesel preparation [17].

The yield of FAME in different periods (20, 40, 60, 90, 120, 150, 180 and 210 min) was measured using a GC-7860 gas chromatograph with KB-Wax capillary column (30 m × 0.32 mm × 0.25 μm) and a flame ionization detector (FID). The temperature program is as follows: the temperature gradient in the range of 100–200 °C with heating rate of 20 °C min^{-1} for 3 min and then increased in the range of 200–220 °C with heating rate of 10 °C min^{-1} for 3 min. At last, the temperature gradient was in the range of 220–0 °C with the heating rate of 10 °C min^{-1} for 3 min. In the investigation of catalytic performance, calcination temperature, mole ratio of nitrate and sodium carbonate, CaO(P) dosage, reaction temperature and ratio of oil, ester, alcohol were presented in detail because of their significant effects on the catalytic capacity. The calculation results of FAME yield were measured in accordance with Eq. (1) to determine the optimum conditions for obtaining CaO(P), where $\sum A_i$, A_{MH}, C_{MH} (1 mg mL^{-1}) and V_{MH} (1 μL) are a symbol of the peak area of the all FAME, the peak area of methyl heptadecanoate, the concentration of the methyl heptadecanoate, the injection volume, respectively. W (mg) is of the quality of product oil:

$$\text{yield}(\%) = \left[\frac{\left(\sum A_i - A_{MH}\right)}{A_{MH}}\right]\frac{C_{MH}V_{MH} \times 100}{W} \quad (1)$$

Chemicals and Materials

All analytical chemicals reagent related to catalyst synthesis and biodiesel preparation such as CH_3COOCH_3 (Kelon Co., Chengdu, China), CH_3OH (Fuyu Co., Tianjin, China), NaOH (Tianli Co., Tianjin, China), C_6H_{12} (Tianli Co., Tianjin, China), $C_{18}H_{38}O_2$ (TCI Co., Shanghai, China), C_2H_5OH (Fuyu Co., Tianjin, China), $Ca(NO_3)_2{\cdot}4H_2O$ (Damao Co., Tianjin, China), Na_2CO_3 (Beilian Co., Tianjin, China) had no further treatment. Rapeseed oil as raw material was obtained from Jianxing Co., Shanxi, China. The chemical and physical properties of rapeseed oil are shown in Table 1. The broken rape pollen (diameter of 30–40 μm, density of 0.6–1.0 g/cm^3) was obtained from Changge Yanyuan Bee

Table 1 Properties of rapeseed oil

Properties	Wt %
Saturated C16 fatty acid	3.7
Saturated C18 fatty acid	1.4
Unsaturated C16:1 fatty acid	61.6
Unsaturated C18:2 fatty acid	21.8
Unsaturated C18:3 fatty acid	0
Density (kg/m^3)	878
Kinematic viscosity (mm^2 /s)	4.13

Products Co., Ltd. Commercial CaO was purchased from Kermel Co., Ltd.

Catalyst Characterization

The structural details of the template CaO(P) were characterized by various characterization techniques. By employment of Micromeritics ASAP 2020 HD88, the BET surface areas and pore-size distribution (PSD) of the CaO(P) were measured based on BET equation and BJH model [18]. It was noted that the thermal properties in range of 25–800 °C of the CaO(P) were collected by TGA-SDTA851 analyzer [19]. As shown by FT-IR, spectra of the CaO(P) in the wavenumber range of 4000–500 cm^{-1} were recorded on Nicolet 5700 by means of KBr pellet technique [20]. Finally, the SEM figures and XRD patterns (2θ: 10°–80°) of the CaO(P) were presented, where they were performed using JSM-6390A [21] and D8 ADVAHCL with Cu-K_α radiation of 40 kV and 30 mA [19].

Catalyst Preparation

The rape pollen (60 g) was cleaned by anhydrous alcohol (90 g) for 1 h under ultrasound for further experiments (step 1). The CaO(P) preparation was carried out by precipitation approach as suggested as follow: 20 g processed pollen was added into calcium nitrate solution (1 mol/L 100 mL) under stirring. After 3 h the suspension was obtained and heated to 70 °C, and then sodium carbonate solution (0.5–1.5 mol/L 100 mL) with the different molar mass as calcium nitrate was added into suspension under continuous stirring and controlled temperature (70 °C) for the formation of calcium carbonate (step 2), following by centrifugation, washing, drying, calcination (600–800 °C) to obtain solid base CaO(P) (step 3) as shown in Fig. 1. The templated CaO(P) were assigned to X-CaO(P)-Y, where "X" was the mole ratio of calcium nitrate to sodium carbonate, "Y" was symbol of the calcination temperature, as well as the expression of "P" was referred to the precipitation method.

Reusability

The reusability of 10 wt% CaO(P) was investigated at same react condition by repeating the transesterification reaction several times with used catalysts. After each reaction, catalysts were separated from the previous reaction mixture by centrifugation, washed with hexane, and then dried at 60 °C and introduced into fresh substrate.

Results and Discussion

Characterization of Catalysts

BET Analysis

For the Tables 2, 3 and Fig. 2a, b, it was depicted the textural details of pores from as-obtained templated CaO(P) calcined in various temperatures range from 600 to 800 °C and the mole ratios of nitrate to sodium carbonate ($n(Ca^{2+}):n(Na_2CO_3)$) between 1/0.5 and 1/1.5. It was seen that the calcination temperature is an important factor affecting the textural properties of CaO (P), and

Table 2 Pore structure properties of derived CaO(P) from different calcination temperature and commercial CaO

Type of catalyst	BET surface area (m^2/g)	Pore volume (cm^3/g)	Average pore diameter (nm)
1/1-CaO(P)-600	10.57	0.03	10.35
1/1-CaO(P)-700	14.92	0.04	11.96
1/1-CaO(P)-800	13.03	0.04	12.63
Commercial CaO-700	11.44	0.03	11.31

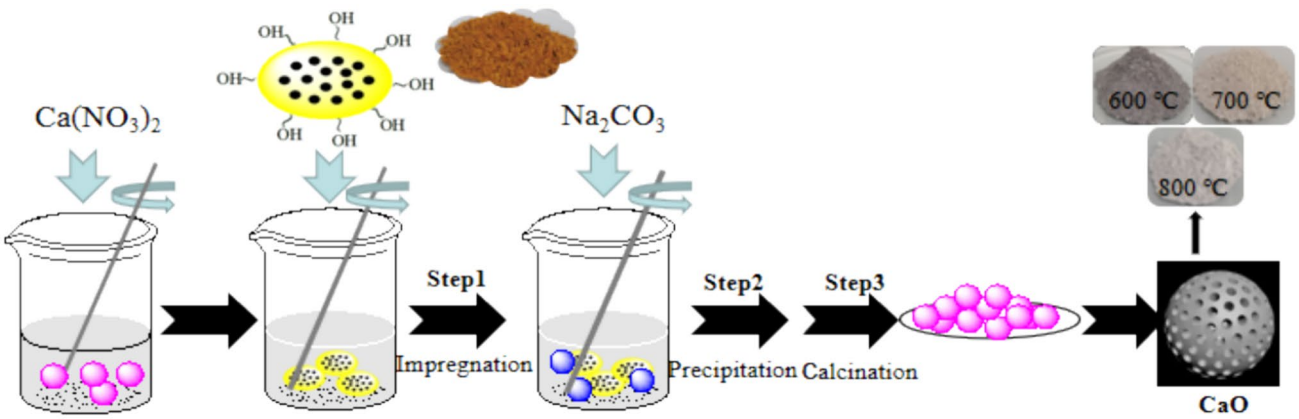

Fig. 1 The preparation pollen-derived CaO

Table 3 Pore structure properties of derived CaO(P) from different proportion of nitrate to sodium carbonate and commercial CaO

Type of catalyst	BET surface area (m^2/g)	Pore volume (cm^3/g)	Average pore diameter (nm)
1/0.5-CaO(P)-700	14.16	0.04	11.97
1/1-CaO(P)-700	14.92	0.04	11.96
1/1.5-CaO(P)-700	10.34	0.02	9.46
Commercial CaO-700	11.44	0.03	11.31

the results showed that BET surface area, pore volume, pore size keep an increase tendency from 10.57 to 14.92 m^2/g, 0.03–0.04 cm^3/g, 10.35–11.96 nm, respectively, as the calcination temperature changed from 600 to 700 °C. However, with the increased calcination temperature to 800 °C, the textural parameters declined as presented by BET surface area of 13.03 m^2/g and pore volume of 0.04 cm^3/g, which attributed the sintering of CaO(P) surface and the reduction in mesopores numbers as shown in Fig. 2.

CaO(P) obtained under different calcination conditions were of a typical IV isotherm with a H3-type hysteresis loop ($P/P_0 > 0.4$) for interpretation of mesopore materials [6]. It could be further confirmed by PSD results centered at 3.5 and 7 nm, indicating the generation of hierarchical structure [22]. Besides, it was also found that 1/1-CaO(P)-700 had best BET surface area (14.16 m^2/g) and pore volume (0.04 cm^3/g) which providing an extensive potential for efficient catalysis of no-glycerol biodiesel and suggested that the higher the sodium carbonate content, the pore plugging leads to the improvement of structural properties.

XRD Analysis

In order to further explore the effect of the preparation conditions of as-obtained CaO(P) powder on its phase composition, the evaluations in this section were the position of diffraction peak of CaO (JCPDS 48-1467), $Ca(OH)_2$ (JCPDS 44-1481) and $CaCO_3$ (JCPDS 33-0268) [23]. The details of diffraction peaks of CaO(P) are presented in Fig. 3a. It can be seen clearly that the calcinating temperature had positive impact on composition of CaO and $Ca(OH)_2$ for reasons of the carbonate decomposition. The crystal planes (111), (200), (202), (311) and (222), meanwhile, were observed at $2\theta = 32.21°$, 37.36°, 53.86°, 64.19° and 67.38° from 1/1-CaO(P)-700 [24] presented to CaO phase. Moreover, it can been found that the relatively sharp and intense diffraction peaks of CaO over 1/1-CaO(P)-700 indicated its better crystallite, while the broad peaks of the commercial CaO-700 indicated its smaller grain size and poor meso–macro-pore distribution according to the Scherrer formula ($D = K\lambda/B\cos\theta$) [25]. However, the relatively sharp diffraction peaks of CaO over 1/1-CaO(P)-800 were an indication of poor dispersion according to the Scherrer formula ($D = K\lambda/B\cos\theta$), which was due to the sintering surface and a decrease in specific surface area, suggesting that a proper calcination temperature was conducive to promote the dispersion of CaO particles so as to its catalytic performance to transesterification reaction [26]. Furthermore, it can be found that the phase of $CaCO_3$ with poor catalytic activity can be discomposed completely when calcination temperature above 600 °C which is well consistent with the thermal analysis result as shown in Fig. 5. Meanwhile, it was found that the molar ratio of nitrate and sodium carbonate is also one of the important factors affecting the morphology, structure and composition of CaO(P) samples. As shown

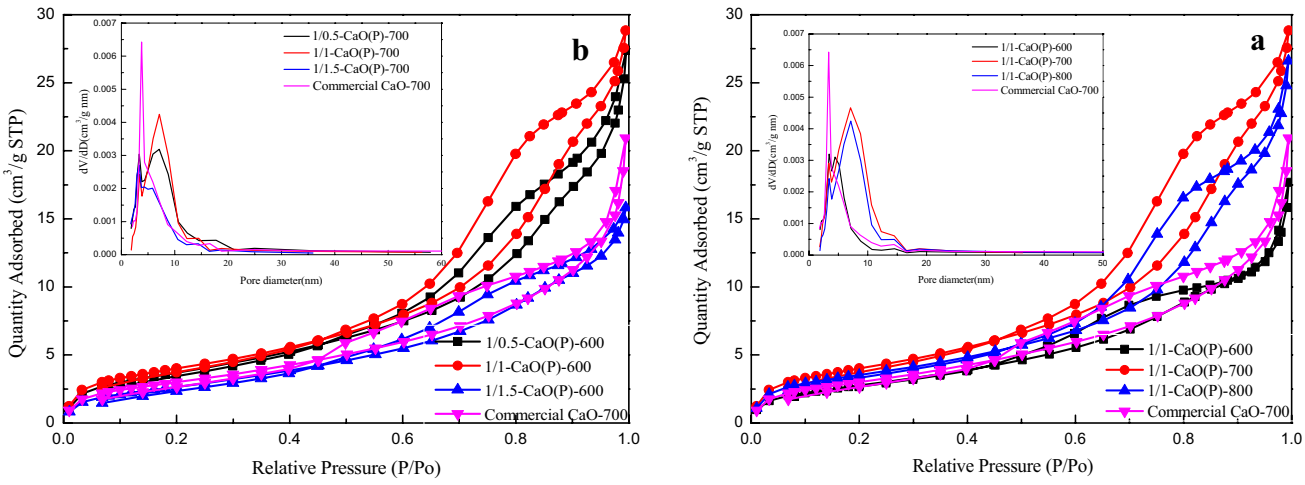

Fig. 2 The N_2-adsorption–desorption isotherms and pore-size distributions (PSD) of the synthesized CaO(P) samples. **a** The calcination temperature; **b** the mole ratio of nitrate and sodium carbonate

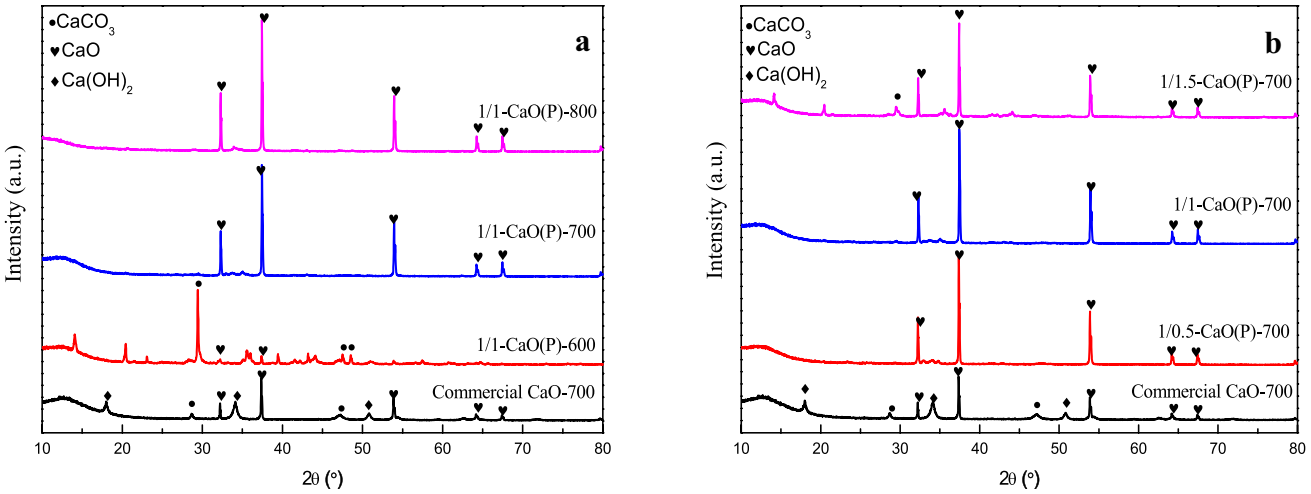

Fig. 3 XRD patterns of the synthesized CaO(P) samples. **a** The calcination temperature; **b** the mole ratio of nitrate and sodium carbonate

in Fig. 3b, with an incremental sodium carbonate (1/1.5-CaO(P)-700), the presence of $CaCO_3$ during the pyrolysis process under 700 °C to the worse catalytic performance accounted for the weak conjugated base of $CaCO_3$.

FT-IR Analysis

FT-IR spectra measurements on the pyrolyzed CaO(P) had offered the more detailed evidences to explain its thermal behavior. Typical FT-IR spectra, for 1/1-CaO(P)-600, 1/1-CaO(P)-700 and 1/1-CaO(P)-800 samples, are presented at Fig. 4a. It was encountered that the stretching vibrations of –OH at 3648, 3448 and 1647 cm^{-1}, respectively [24], due to the hydroxyls groups from the physisorbed water molecules in materials [27]. Meanwhile, the sharp-pointed bands of carbonate were seen from the wave number of 1459, 871 and 713 cm^{-1} [28]. Further an advancement in calcinations temperature from 600 to 800 °C, the intensity of two types of bands started getting a little smaller and weaker, which was due to the full thermal decomposition of generated precipitation $CaCO_3$. Furthermore, the increasingly sharp vibration band of CO_3^{2-} was observed in as-obtained 1/1-CaO(P)-600 sample, suggesting that the calcination temperature of 600 °C was supposed to incompletely remove carbonate. While it was significant to comprehend that the increased temperature (700 °C) promoted to the ameliorated diffusivity leading to faster crystallization of CaO and then the shrinkage was prevented. Figure 4b shows that the CaO(P) samples calcined at 700 °C with different sodium carbonate contents consist of CaO, $Ca(OH)_2$ and $CaCO_3$, and it can be seen from the figure that sharp carbonate bands can be seen from the wave numbers of 1459, 871 and 713 cm^{-1}, which

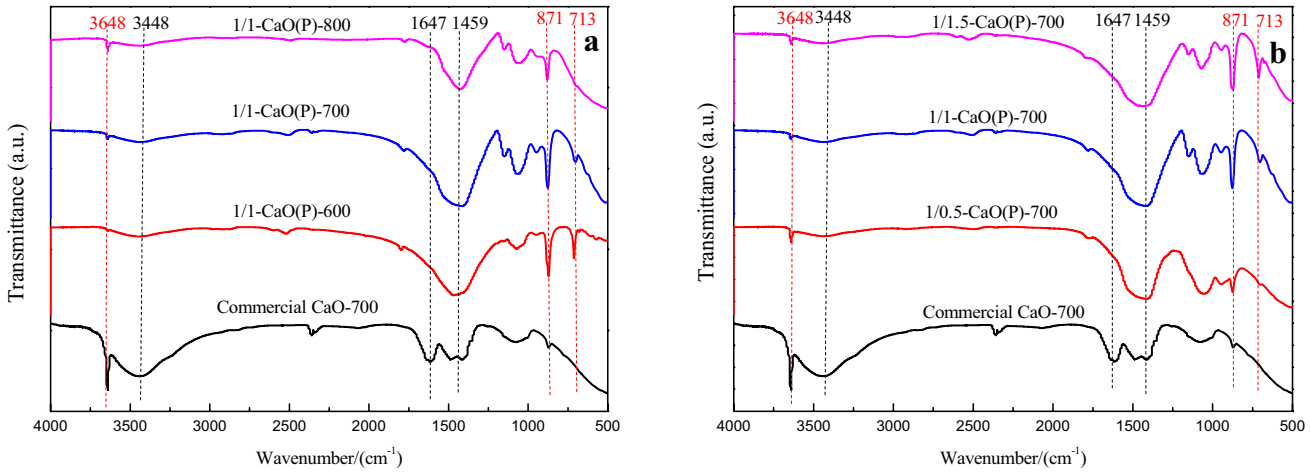

Fig. 4 FT-IR spectra of the synthesized CaO(P) samples. **a** The calcination temperature; **b** the mole ratio of nitrate and sodium carbonate

become larger and stronger as the amount of sodium carbonate increases due to the generated more precipitate $CaCO_3$.

TG Analysis

TG and DTG curves of the as-synthesized CaO(P) samples after various calcination treatment are presented in Fig. 5a, b. It was observed that there were one major weightloss interval assigned to the pyrolyzation of $CaCO_3$, which was visible in 510–790 °C with the weight loss value of 26%, 6% and 2%, expressed by 1/1-CaO(P)-600, 1/1-CaO(P)-700 and 1/1-CaO(P)-800, respectively. Conversely, commercial CaO-700 had two decomposition intervals corresponding to decomposed $Ca(OH)_2$ and $CaCO_3$ at 330–400 °C and 510–790 °C, as well as the more weightlessness was observed (13%). For a series of CaO(P) materials derived from nitrate and sodium carbonate with mole ratio of 1/1 under different calcination temperatures, a shift to higher temperature could be seen with calcination temperature from 600 to 800 °C, which maybe indicated the stronger stability as well as avoidance from the impact of the air [29]. Certainly, the more obvious weight loss of $CaCO_3$ was observed (Fig. 5c, d) due to sodium carbonate consumption. It should be mentioned, however, that the weightlessness of 1/0.5-CaO(P)-700, 1/1-CaO(P)-700 and 1/1.5-CaO(P)-700 were reflected in 4%, 6% and 13%. From the result it can be observed that all of sample can be transformed to CaO after calcined above 510 °C and an increase in the weightloss of $CaCO_3$ with the higher concentration of CaO(P) (calcium nitrate/sodium carbonate), due to the generation of more precipitation or severe corrosion by air. Therefore, the CaO(P) samples over an appropriate pyrolysis temperature (700 °C) and the addition amount of sodium carbonate (1/1) was comparatively favorable to obtain well dispersion and stability CaO particles.

CO_2-TPD Analysis

The CO_2-TPD curves of CaO(P) under different calcination conditions are shown in Fig. 6a. It can be seen that

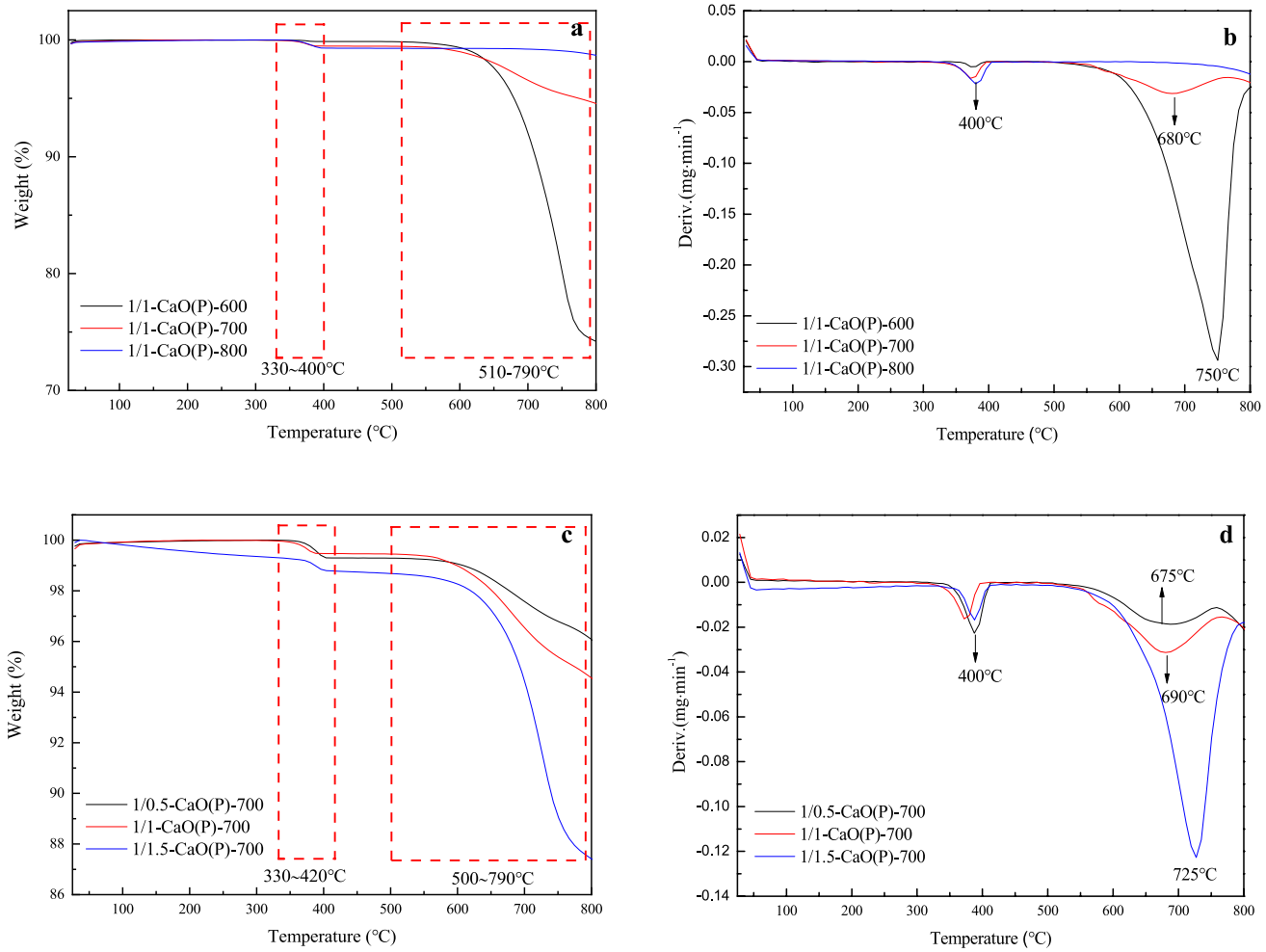

Fig. 5 TG curves of the synthesized CaO(P) samples. **a**, **b** The calcination temperature; **c**, **d** the mole ratio of nitrate and sodium carbonate

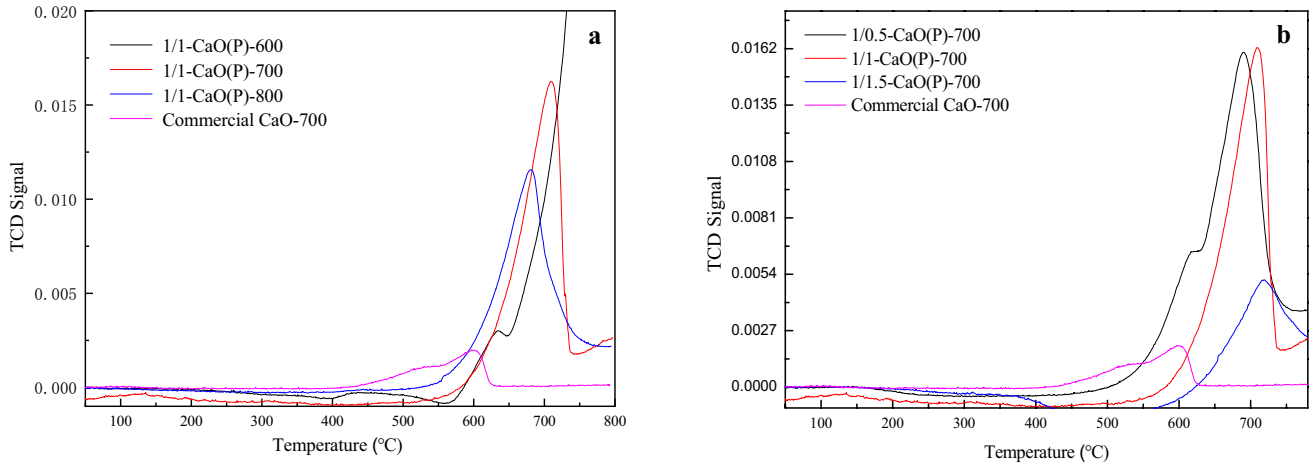

Fig. 6 CO_2-TPD curves of the synthesized CaO(P). **a** Calcination conditions; **b** the mole ratio of nitrate and sodium carbonate

the CO_2-TPD curves with a single peak were presented by CaO(P), and the CO_2-desorption temperature appeared around 700 °C, suggesting that CaO(P) had strong basic site. When $n(Ca^{2+}):n(Na_2CO_3) = 1/1$, the CO_2-TPD curve of CaO(P) shifted to right and the peak area gradually increased so as to the highest total basicity (4.48 mmol/g) as the calcination temperature increases from 600 to 700 °C. However, it was found that the surface of the 1/1-CaO(P)-800 had 13.03 m^2/g (BET specific surface area) after sintering, which caused its total basicity to drop to 3.37 mmol/g. As seen in Fig. 6b, it can be observed that when $n(Ca^{2+})/n(Na_2CO_3)$ increased from 1/0.5 to 1/1, the total basicity of CaO(P) were calculated to 4.00 and 4.48 mmol/g, respectively, which was attributed to the hydrolysis of Na_2CO_3 in aqueous solution to generate CO_3^{2-} and OH^-, followed by reaction with Ca^{2+} to form $CaCO_3$ and $Ca(OH)_2$, thus effectively avoiding the precipitation of Ca^{2+}. Besides, the increase of BET specific surface area was beneficial to the change of total basicity as result of the increase of surface basic sites [30]. A large amount of $CaCO_3$ and $Ca(OH)_2$ were produced on the pollen surface as $n(Ca^{2+})/n(Na_2CO_3)$ was 1/1.5, which reduced the BET specific surface area of 1/1.5-CaO(P)-700 to 10.34 m^2/g so as to the decreased total basicity (1.36 mmol/g). Therefore, 700 °C of calcination and 1/1 of $n(Ca^{2+})/n(Na_2CO_3)$ were selected as the optimal preparation conditions for CaO(P) [31] (Table 4).

Table 4 Total basicity of CaO(P) and Commercial CaO-700

Type of catalyst	Total basicity (mmol/g)	Desorption peaks (area%)
1/1-CaO(P)-600	–	–
1/1-CaO(P)-700	4.48	1.04
1/1-CaO(P)-800	3.37	0.78
1/0.5-CaO(P)-700	4.00	0.93
1/1.5-CaO(P)-700	1.36	0.32
Commercial CaO-700	0.79	0.18

SEM Analysis

The SEM pictures of the original pollen, pretreated pollen (Fig. 7a, b), synthesized CaO(P) samples (Fig. 7c–g), as well as commercial CaO prepared under 700 °C (Fig. 7h) had been shown. It was conspicuous that the microstructure of the original pollen was similar to ultrasonic treated pretreated pollen with germination holes and germination grooves. However, it was clearly seen that the collapse of the 3D structure after the high temperature pyrolysis [32]. Figure 7c–e depicts images of CaO(P) calcined in the temperature range of 600–800 °C, where the degree of calcination agglomeration becomes increasingly apparent as the temperature increases. It can be seen that the samples calcined at 800 °C were agglomerated and sintered on the surface with lower yields, while at 600 and 700 °C, the particle size distribution was uniform with good dispersion. Meanwhile, it was important to find the significant differences of morphology in the three templated CaO(P) pyrolyzed calcined at 700 °C from several mole ratio, 1/0.5, 1/1 and 1/1.5 of nitrate to sodium carbonate, as presented in Fig. 7f, d and g. It was found that when the molar ratio were 1:0.5 and 1:1.5, the CaO crystal particles aggregated into lumps with poor dispersion at insufficient or excessive amount of sodium carbonate. The experimental results showed that the dispersion of CaO(P) particles were not only temperature dependent, but also the amount of sodium carbonate was a key factor, and it was observed that the best dispersion performance was obtained at 700 °C and 1/1.5.

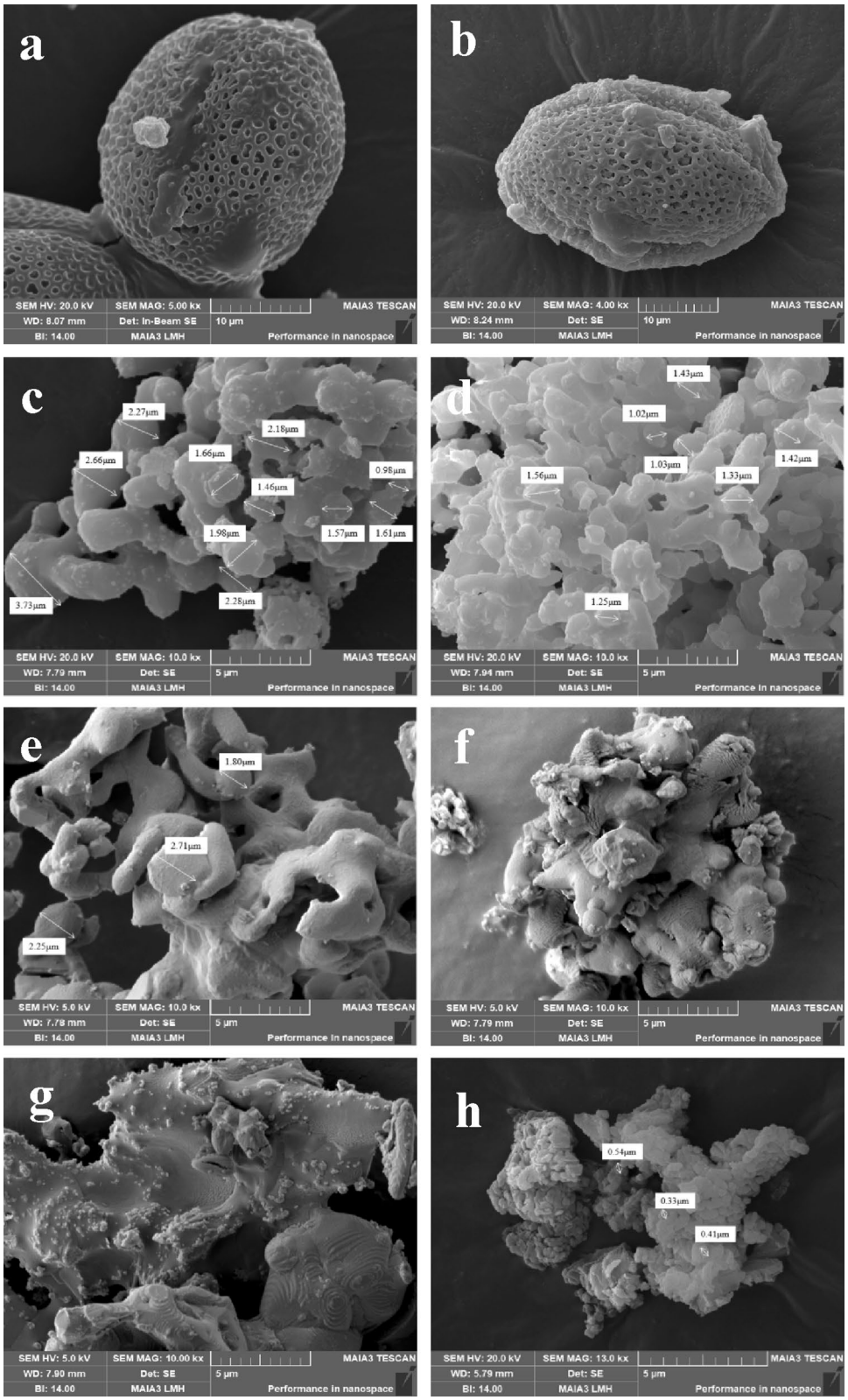

Fig. 7 SEM pictures of the synthesized CaO(P) samples. **a** The original pollen; **b** pretreated pollen; **c** 1/1-CaO(P)-600; **d** 1/1-CaO(P)-700; **e** 1/1-CaO(P)-800; **f** 1/0.5-CaO(P)-700; **g** 1/1.5-CaO(P)-700; **h** commercial CaO

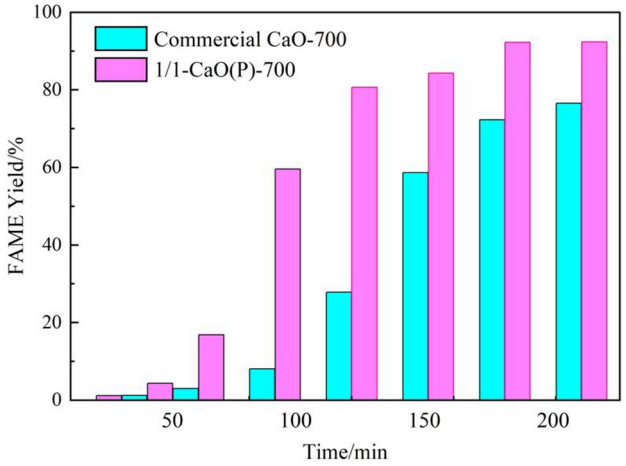

Fig. 8 Comparison of templated 1/1-CaO(P)-700 and commercial CaO-700

No-glycerol Biodiesel Preparation

Comparison of Catalytic Properties

Interesting distinctions of FAME yield regularity had been drawn between as-synthesized 1/1-CaO(P)-700 and commercial CaO-700 as depicted in Fig. 8. In a typical reaction, the mixture consisting of 1 mol rapeseed oil (960 g mol^{-1}), 1 mol methyl acetate and 8 mol anhydrous methanol were magnetically stirred in a 65 °C water bath with the participation of the commercial CaO-700 or 1/1-CaO(P)-700 (10 wt %). As shown, over 3 h, the FAME yield over templated 1/1-CaO(P)-700 material can be obtained more than 90% which is better than over commercial CaO with less than 80%. It indicates that the templated CaO(P) material provides more active sites which provide a great opportunity to increase the rate of transesterification reaction [33].

Effect of Preparation Parameters on FAME Yield

The yield of no-glycerol biodiesel generally refers to the content of fatty acid methyl ester (FAME) that determined over a gas chromatography by testing for the product. Accordingly, the FAME yield is an important parameter for the catalytic performance of solid base. Calcination is the most critical step in the preparation of template CaO(P) and is the most important step affecting its catalytic properties, as manifested in alkalinity strength, phase composition and pore-size distribution. The chemical and physical properties of FAME are shown in Table 5. The effect of resulting CaO(P) samples calcinated in range from 600 to 800 °C on FAME yield had been seen in Fig. 9a, implying that the catalytic performance of 1/1-CaO(P)-700 was effective, which was due to the formation of dispersed CaO from lower

Table 5 Fuel properties of FAME

Properties	Test method	EN14214
Relative density, 298 K	0.89	0.86–0.90
Viscosity, 313 K (mm^2 /s)	4.6	3.5–5.0
Flashpoint (K)	437	> 373
Ester content (%)	91.8–99.8	96.5
Free glycerol (%, m/m)	0.02	< 0.02

calcination temperature, however, the reduction of the specific surface area (SSA) on catalyst surface for agglomeration and sintering over higher calcination temperature [31]. Simultaneously, the transesterification was carried out in 1/1/8 (oil/ester/alcohol) mixture under stirring for 3 h, which showed that the addition of 10 wt% 1/1-CaO(P)-700 resulted in a considerable increase in FAME yield (92.69%) at 65 °C. Nevertheless, the catalytic behaviors of 1/1-CaO(P)-600 and 1/1-CaO(P)-800 were obviously weakened, yielding to no-glycerol biodiesel of 2.23% and 85.65%, respectively.

To determine the optimum mole ratio of nitrate and sodium carbonate of CaO(P), the effect of the amount of sodium carbonate on FAME yield was visualized as shown in Fig. 9b. As shown, the catalytic effect of CaO(P) (dosage: 10 wt%) in the mixed solvent (1/1/8 rapeseed oil–methyl acetate–methanol) increased from 74.69 to 92.69% after 3 h at 65 °C, which attributed that a growing number in sodium carbonate was conducive to the formation of more active ingredients such as CaO. Besides, it should be noted that the FAME yield over 1/1.5-CaO(P)-700 could only reach 73.80% (Fig. 9b) due to the accumulation of a large amount of calcium salt deposits on the template, which further affecting the porous structure of the obtained solid base CaO(P).

Effects of Reaction Parameters on FAME Yield

The amount of templated CaO(P) had a significant effect on catalytic efficiency of transesterification, which was investigated in Fig. 10a. It was observed that the variation of FAME yield at different dosages of 1/1-CaO(P)-700 sample in the presence of mixed solution composed of 1/1/8 oil/methyl acetate/methanol at 65 °C for 3 h. As expected, the FAME yield grew from 12.25 to 92.69% as the number of CaO(P) increased from 5 to 10 wt%, which was in agreement with other reported studies that more provision of active sites resulted in the easier attraction of triglyceride molecules and methanol to recombination [34]. On the contrary, the catalytic effect is greatly reduced by an excess of CaO(P), which was related to the increase in the viscosity of the reaction and the generation of side reactions such as saponification, expressed in the yield of 54.31% at 15 wt% CaO(P) [35]. In conclusion, the following series of

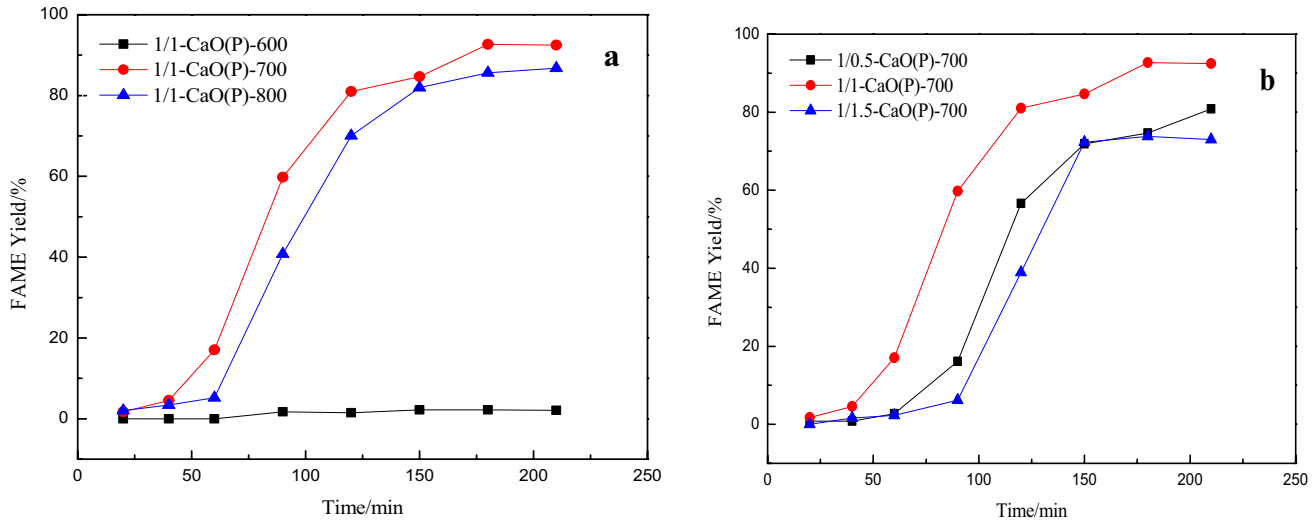

Fig. 9 Effect of templated CaO(P) preparation parameters on yield. **a** The calcination temperature; **b** the mole ratio of nitrate and sodium carbonate

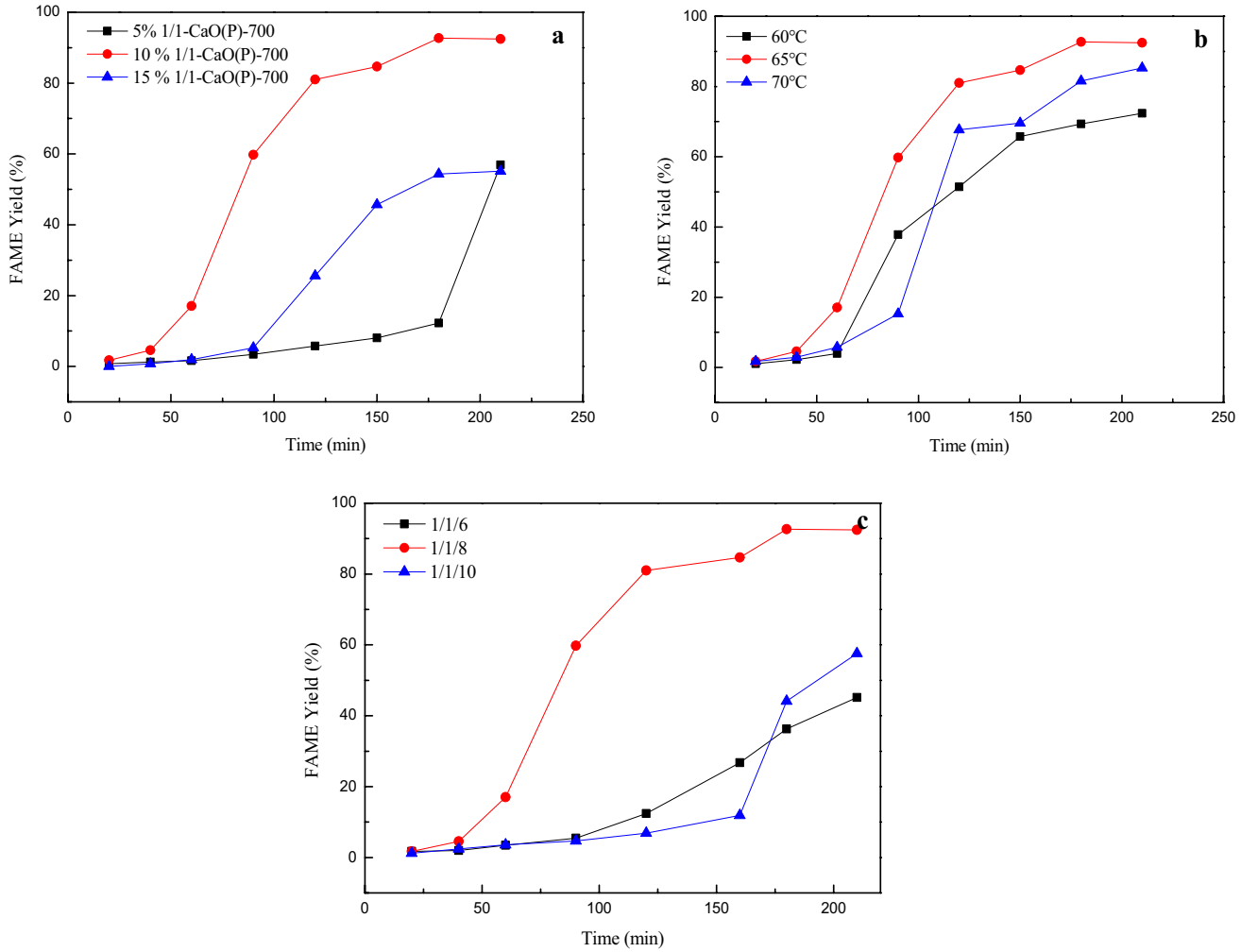

Fig. 10 Effects of reaction parameters on FAME yield. **a** The catalyst amount; **b** the reaction temperature; **c** the oil/ester/alcohol ratio

experimental research will be conducted at the addition of 10 wt% CaO(P).

Within these selected parameters, the reaction temperature, as a representative, affecting FAME yield was especially prominent, and the positive correlation relationship between FAME yield and reaction temperature in certain range was available due to its classification of endothermic reaction [36]. In this section, the empirical results proposed in Fig. 10b are cited to determine the optimal value of reaction temperature. Comparison of the measured curves of 10 wt% 1/1-CaO(P)-700 in three mixed reagents (1/1/8: oil/methyl acetate/methanol) under 60, 65, 70 °C, respectively, it can be observed that the FAME yield can reach 92.69% after 3 h under 65 °C, nevertheless, methanol could be vaporized to its lower content in the solution under higher reaction temperature (70 °C), which was detrimental to the forward movement of the equilibrium reaction [37], resulting in a decrease in the yield of biodiesel, expressed as 81.60%.

Contrary to traditional injected quantity of methanol with 1/3 mol L^{-1} ratio of oil/alcohol, methanol were customarily arranged by overdose, reflected 1/15 mol L^{-1} ratio. The varied molar ratio of oil–methyl acetate–methanol was examined under optimized factors containing temperature of 65 °C and the dosage of 10 wt%, executed by 1/1-CaO(P)-700, which were shown in Fig. 10c. Since the increase in the amount of methanol for the reversible esterification reaction contributed to increase the reaction rate and accelerate the reaction process, it can be seen that the FAME yield shot up to 92.69% at 1/1/8. However, the ratio was increased to 1/1/10, the FAME yield decreased to 44.15% due to dilution caused by large amounts of methanol [38].

Reutilization Experiments

The reusable property of commercial CaO and 10 wt% CaO(P) was investigated under the optimum reaction condition (Fig. 11). The results showed that the yield of FAME over the modified catalyst was enhanced to nearly 95%. The catalyst maintained sustaining activity even after being used for six cycles and the FAME yield slightly decreased due to the sensitivity of the catalyst to water and/or CO_2 in the reaction.

Conclusion

In this work, a biotemplated methodology for the fabrication of hierarchically porous CaO has been established using pollen as biotemplate. Its catalytic performance in tri-component coupling transesterification (rapeseed oil–methyl acetate–methanol), where the yield of no-glycerol biodiesel was investigated. It was found that the as-obtained CaO(P) catalyst can be used as an effective and recyclable solid basic catalyst and exhibits higher catalytic activity than the commercial CaO powder sample. This is due to hierarchical structure of the biomorphic framework along with a high specific surface area and wide pore-size distribution including mesopores and macropores which promoted alternatives in mass transportation in this heterogeneous reaction. Our study demonstrates an exciting preparation method for higher dispersion catalyst with greatly potential in the fields of catalysis.

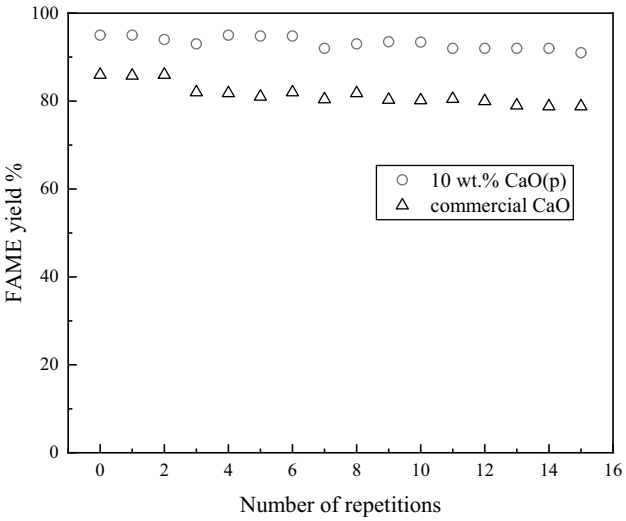

Fig. 11 FAME yield upon transesterification of rapeseed oil for repeated use of commercial CaO and 10 wt% CaO(P) at a reaction temperature of 65 °C, a reaction time of 3 h, and a oil: methyl acetate: methanol ratio of 1:1:8

Acknowledgements The work was supported financially by the National Natural Science Foundation of China (51974252), Scientific Research Program Funded by Shaanxi Provincial (Program No. 2023-YBGY-052) and the Youth Innovation Team of Shaanxi University. In addition, we thank the work of Modern Analysis and Testing Center of Xi'an Shiyou University.

Data availability The data supporting this study's findings are available from the corresponding author upon reasonable request.

References

1. H. Hong, M. Wang, X. Zhang et al., Projection of energy use and greenhouse gas emissions by motor vehicles in China: policy options and impacts. Energy Policy **43**, 37–48 (2012)
2. M.M. Roy, M.S. Islam, M.N. Alam, Biodiesel from crude tall oil and its NO_x and aldehydes emissions in a diesel engine fueled by biodiesel-diesel blends with water emulsions. Processes **9**(1), 126 (2021)
3. N. Mansir, S.H. Teo, N.A. Mijan et al., Efficient reaction for biodiesel manufacturing using bi-functional oxide catalyst. Catal. Commun.. Commun. **149**, 106201 (2021)
4. Y. Tang, H. Liu et al., Tri-component coupling transesterification for efficient no-glycerol biodiesel production using methyl acetate

as methyl reagent. J. Chem. Technol. Biotechnol. **95**, 1234–1242 (2020)
5. B. Mauro, G. Giuseppe, A simple pseudo-homogeneous reversible kinetic model for the esterification of different fatty acids with methanol in the presence of amberlyst-15. Energies **11**(7), 1843 (2018)
6. Y. Tang, Y. Yang, H. Liu et al., Preparation of nano-CaO and catalyzing tri-component coupling transesterification to produce biodiesel. Inorg. Nano-Met. Chem. **50**(7), 501–507 (2020)
7. S. Martins, N. Tapanes, G.R. Orlandini, Study of the properties of an epoxy adhesive with additions of a residue from the biodiesel production process. Int. J. Adhes. Adhes. **103**, 102701 (2020)
8. Y. Tang, H. Liu, H.M. Ren, Development KCl/CaO as a catalyst for biodiesel production by tri-component coupling transesterification. Environ. Prog. Sustain. Energy **38**, 647–653 (2018)
9. P. Hariprasath, S.T. Selvamani, M. Vigneshwar et al., Comparative analysis of cashew and canola oil biodiesel with homogeneous catalyst by transesterification method. Mater. Today Proc. **16**, 1357–1362 (2019)
10. S.J. Chen, I.C. Kuan, Y.F. Tu et al., Surfactant-assisted in situ transesterification of wet *Rhodotorula glutinis* biomass. J. Biosci. Bioeng. **130**(4), 7–401 (2020)
11. C. Quan, N. Gao, H. Wang et al., Ethanol steam reforming on Ni/CaO catalysts for coproduction of hydrogen and carbon nanotubes. Int. J. Energy Res. **43**(3), 1255–1271 (2019)
12. D. Ramimoghadam, M. Hussein, T.Y. Yun, Synthesis and characterization of ZnO nanostructures using palm olein as biotemplate. Chem. Cent. J. **7**(1), 71 (2013)
13. M.A. Faramarzi, A. Sadighi, Insights into biogenic and chemical production of inorganic nanomaterials and nanostructures. Adv. Coll. Interface. Sci. **189–190**(3), 1–20 (2013)
14. A.H. Cheng, Q.Y. Xie, Preparation of Fe-based composites based on rape pollen template and their catalytic properties. Mater. Guide **37**(21), 1–11 (2023)
15. C. Chen, R.Y. Bao, J.X. Xia et al., Synthesis and properties of rare earth doped TiO_2 with plant pollen as template. Chin. J. Rare Earths **37**(5), 602–608 (2019)
16. J. Chen, H. Zou, R. Liu et al., Synthesis of nanomaterials by high gravity reactive precipitation method and applications. Mod. Chem. Ind. **21**(9), 9–12 (2001)
17. Y. Tang, Y.Y. Xue, Z.Y. Li et al., Heterogeneous synthesis of glycerol carbonate from glycerol and dimethyl carbonate catalyzed by LiCl/CaO. J. Saudi Chem. Soc. **23**(4), 494–502 (2019)
18. T.L. Zhao, T.X. Fan, D. Zhang, Synthesis of biomorphous nickel oxide from a pinewood template and investigation on a hierarchical porous structure. J. Am. Ceram. Soc. **89**, 662–665 (2005)
19. A. Hemalatha, S. Arulmani, E. Chinnasamy, Synthesis, growth and characterization of new nonlinear optical material of L-Norvalinium hydrogen maleate. Mater. Today Proc. **34**(1), 412 (2020)
20. M. Hayati-Ashtiani, Characterization of nano-porous bentonite (montmorillonite) particles using FTIR and BET-BJH analyses. Part. Part. Syst. Charact. **28**(3–4), 71–76 (2012)
21. Y. Tang, Z.Y. Li, Z.Y. Xu, Synthesis of hierarchical MgO based on a cotton template and its adsorption properties for efficient treatment of oilfield wastewater. RSC Adv. **10**(48), 28695–28704 (2020)
22. E. Fayyazi, B. Ghobadian et al., Intensification of continues biodiesel production process using a simultaneous mixer-separator reactor. Energy Sources Recov. A Util. Environ. Effects **40**(9), 1125–1136 (2018)
23. C.Z. Yuan, X.G. Zhang et al., Synthesis and electrochemical capacitance of mesoporous $Co(OH)_2$. Mater. Chem. Phys. **101**(1), 148–152 (2007)
24. A. Knk, B. Sns, C. Csak, Optimization and kinetic study of biodiesel production from *Hydnocarpus wightiana* oil and dairy waste scum using snail shell CaO nano catalyst. Renew. Energy **146**, 280–296 (2020)
25. E. Costa, M.F. Almeida, M. Alvim-Ferraz et al., Effect of *Crambe abyssinica* oil degumming in phosphorus concentration of refined oil and derived biodiesel. Renew. Energy **124**, 27–33 (2018)
26. C.L. Yao, M.X. Hu, B.Y. Han et al., Mineralization of calcium carbonate induced by pollen as template. J. Chongqing Inst. Sci. Technol. **22**(04), 53–58 (2020)
27. Y.F. Yang, *Research on Electrochemical Properties of the Lotus Pollen-Derived Porous Carbons and Its Composites* (Jiangsu University, China, 2021)
28. W.W. Mar, E. Somsook, Methanolysis of soybean oil over KCl/CaO solid base catalyst for biodiesel production. ScienceAsia **38**(1), 90–94 (2012)
29. W. Zeng, *Sunflower Pollen–Biotemplated Synthesis of Hierarchically Porous Zirconia Toward 1,3-Butadiene Selective Hydrogenation* (Xiamen University, China, 2020)
30. Y.H. Xiao, L. Li et al., Synthesis of mesoporous ZnO nanowires through a simple in situ precipitation method. Nanotechnology **16**(6), 671–674 (2005)
31. Z.X. Huang, L.X. Chen, P.T. Wang et al., Lanthanum-doped solid base MgO/SBA-15 catalysed biodiesel preparation from soybean oil. New Chem. Mater. **48**(03), 232–235 (2020)
32. Y.C. Wong, Y.P. Tan et al., Effect of calcination temperatures of CaO/Nb_2O_5 mixed oxides catalysts on biodiesel production. Sains Malays. **43**(5), 783–790 (2014)
33. A.P. Shi, J.M. Zhu, Q. Ma, Biodiesel preparation with solid base catalyst under ultrasonic assistant. Appl. Mech. Mater. **548**, 158–163 (2014)
34. B. Sutrisno, A.D. Nafiah, I.S. Fauziah, CaO/natural dolomite as a heterogeneous catalyst for biodiesel production. Mater. Sci. Forum **6079**, 117–122 (2020)
35. K.T. Tan, K.T. Lee, A.R. Nohamed, Optimization of supercritical dimethyl carbonate (SCDMC) technology for the production of biodiesel and value-added glycerol carbonate. Fuel **89**, 3833–3839 (2010)
36. N. Kaur, A. Ali, One-pot transesterification and esterification of waste cooking oil via ethanolysis using Sr: Zr mixed oxide as solid catalyst. RSC Adv. **4**(82), 43671–43681 (2014)
37. Dianursanti, M. Delaamira, S. Bismo, Effect of reaction temperature on biodiesel production from *Chlorella vulgaris* using CuO/zeolite as heterogeneous catalyst. IOP Conf. Ser. Earth Environ. Sci. **55**(1), 012033 (2017)
38. Y. Kojima, S. Takai, Transesterification of vegetable oil with methanol using solid base catalyst of calcium oxide under ultrasonication. Chem. Eng. Process. **136**, 101–106 (2018)